

Design of Two Resistors Loaded Ultra-Wideband Spiral Array Antennas

Satoshi Yamaguchi ¹, Hiroaki Miyashita ¹, Kazushi Nishizawa ¹,
Kenichi Kakizaki ¹, Shigeru Makino ¹,
¹ Mitsubishi Electric Corporation
5-1-1 Ofuna, Kamakura, Kanagawa 247-8501, Japan
Yamaguchi.Satoshi@ce.MitsubishiElectric.co.jp

1. Introduction

Spiral antennas [1][2] have ultra-wideband characteristics such as a nearly constant input impedance, antenna gain, and low axial ratio. However, when reflectors such as conducting planes or cavities are used, their performances are degraded due to reflections from the end of their spiral arms [3]. In particular, this effect is remarkable at low frequencies where these antennas become small in comparison to their wavelengths. Therefore, some techniques to improve the characteristics of spiral antennas are reported [4][5]. In this paper, we propose a new type of a small spiral antenna that has a pair of resistors and verify its ultra-wideband characteristics. Also, we show the array antenna performances through numerical simulations by using the FDTD method.

2. Design of Two Resistors

A square spiral antenna that is composed of two arms is illustrated in Fig. 1. Its outer circumference is $0.96\lambda_L$, and its cavity depth is $0.09\lambda_L$. The antenna is fed at the center of the spiral, and a wideband tapered balun formed by using a microstrip line is used for impedance matching.

The following two electric modes that exist at the spiral truncation section are considered. One is an odd mode existing between the tips of the spiral arm and the adjoined spiral arm, and the other is an even mode between the tips of the spiral arm and the ground conductor (cavity). To suppress these two modes, we use a resistor R_o for the odd mode and a resistor R_e for the even mode, as shown in Fig. 1. Land is placed at the opposite side of the resistor R_e connection, and the land and cavity are shorted via a through hole.

The two resistors are chosen in the following manner. The point of the spiral truncation is replaced by a coupled microstrip line, as shown in Fig. 2 and 3. The width and the interval S between the two lines and the height H from the ground conductor is set similarly to the spiral antenna. Fig. 2 and Fig. 3 show the FDTD calculation model for the odd and even modes, respectively. These two lines are fed at one side, and the other sides are inserted in the PML absorbing boundary condition; they become equivalently infinite. To prevent the influence of the feeding structure in calculating the characteristic impedance of the line, the observation point of the voltage and current is set in a position that is sufficiently distant from the feeding point. The subscripts "inc" and "obs" show the feeding and observation points, respectively. Fig. 4 shows the calculation result. The even and odd mode characteristic impedances are $Z_e = 300 \Omega$ and $Z_o = 50 \Omega$, respectively.

For the even mode, the resistor R_e should be equal to Z_e . Although a resistor R_o is undetermined here, the even mode is unaffected by R_o because both strips are at the same potential and no current flow occurs. For the odd mode, it is considered that an electric wall equivalently exists in the middle of the two strips. When an electric wall is assumed to be a potential basis, R_e , determined above, and $R_o/2$ are connected in parallel at the tip of the spiral arm. Thus, the resistor R_o is determined from the following equation:

$$1/Z_o = 1/R_e + 1/(R_o/2) \quad (1)$$

In this manner, R_e and R_o are determined to be 300Ω and 120Ω , respectively.

3. Experimental Results

We fabricated the antenna element based on the design procedure described above, and the measurement results are presented here. Fig. 5 shows the VSWR performance versus frequency (normalized by f_L), and Fig. 6 shows the axial ratio versus frequency. In both figures, the case with and without two resistors are compared. It is seen that two resistors are effective from f_L to $2f_L$ in the case of VSWR and from f_L to $3f_L$ in the case of the axial ratio. In particular, the effect of using two resistors on the axial ratio is significant and an ultra-wideband characteristic is obtained.

Next, the antenna gain frequency characteristic is shown in Fig. 7. It is seen that the antenna gain has hardly changed regardless of the presence of the resistors. Thus, it can be said that the antenna gain does not decrease even if the two resistors are used. This is because the resistors only remove the residual power that does not contribute to the radiation.

4. Array Antenna Performances

In this section, we show the array antenna performances through numerical simulations by using the FDTD method. Fig. 8 shows the layout of the array antenna examined here. The size of the circular aperture is $1.6\lambda_L$ in diameter, and it has 20 elements (5 elements in one quadrant). The lattice of the array is adjusted to an equilateral triangle with a side $0.28\lambda_L$ long, and therefore, the outer circumference of the square spiral antenna is reduced to $0.86\lambda_L$.

Fig. 9, 10 and 11 show the radiation pattern at the frequency of f_L , $2f_L$, $3f_L$ (yz -plane in Fig. 8), respectively. The theoretical result in which the array element pattern is calculated as a cosine shaped electric field is also shown in the figure. Both agree well, and the pattern shape obtained is identical to the theoretical result. Other planes also show similar results. Fig. 12 shows the antenna gain and the axial ratio of the array antenna versus frequency. The antenna gain has decreased near the lowest operating frequency f_L because of the decrease in the size of the spiral antenna. On the other hand, above a frequency of $1.2f_L$ in which the outer circumference is longer than 1λ , it is understood that the antenna gain becomes high and is close to the theoretical result. Further, the axial ratio is below 5 dB in triple bandwidth and the array antenna shows a good performance.

5. Conclusions

We proposed a new termination technique for small spiral antennas backed by a cavity. We showed the design procedure and experimentally verified their ultra-wideband characteristics. Moreover, we examined their array antenna performances and showed that high gain and low axial ratio characteristics were obtained.

References

- [1] W. L. Curtis, "Spiral antennas," *IRE Trans. Antennas Propagat.*, vol. AP-8, pp. 298-306, May 1960.
- [2] J. A. Kaiser "The Archimedean two-wire spiral antenna," *IRE Trans. Antennas Propagat.*, vol. AP-8, pp. 312-323, May 1960.
- [3] H. Nakano, K. Nogami, S. Arai, H. Mimaki, and J. Yamauchi, "A spiral antenna backed by a conducting plane reflector," *IEEE Trans. Antennas Propagat.*, vol. AP-34, no. 6, pp. 791-796, June 1986.
- [4] J. J. H. Wang and V. K. Tripp, "Design of multioctave spiral-mode microstrip antennas," *IEEE Trans. Antennas Propagat.*, vol. 39, no. 3, pp. 332-335, Mar. 1991.
- [5] C. W. Penney and R. J. Luebbers, "Input impedance, radiation pattern, and radar cross section of spiral antennas using FDTD," *IEEE Trans. Antennas Propagat.*, vol. 42, no. 9, pp. 1328-1332, Sept. 1994.

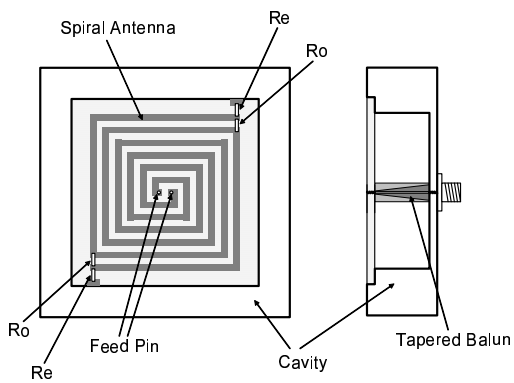


Figure 1: Two resistors loaded spiral antenna backed by a cavity

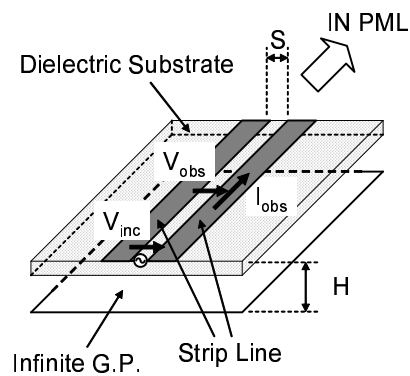


Figure 2: FDTD calculation model of a coupled microstrip line for the odd mode

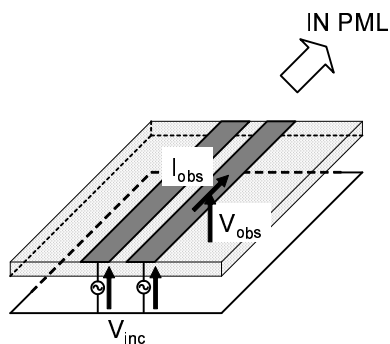


Figure 3: FDTD calculation model of a coupled microstrip line for the even mode

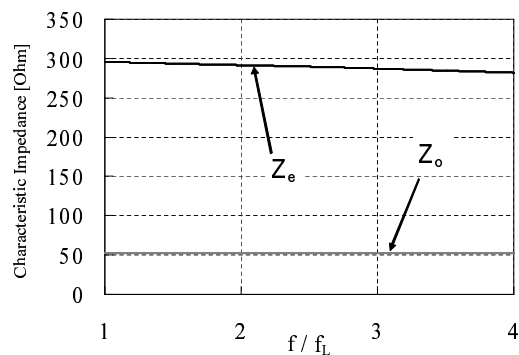


Figure 4: Characteristic impedance of a coupled microstrip line

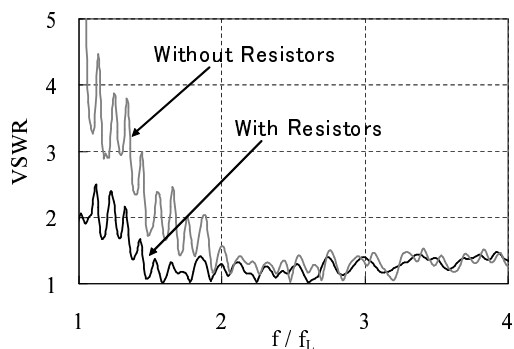


Figure 5: VSWR

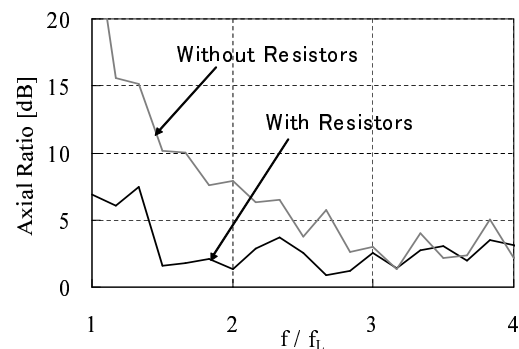


Figure 6: Axial ratio

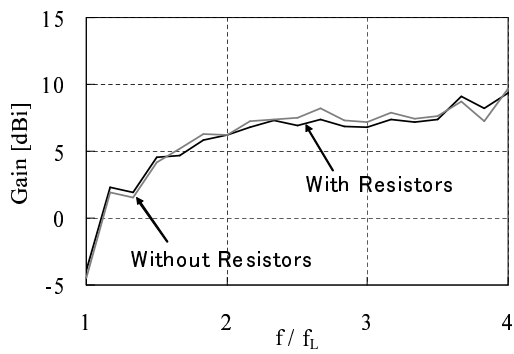


Figure 7: Antenna gain

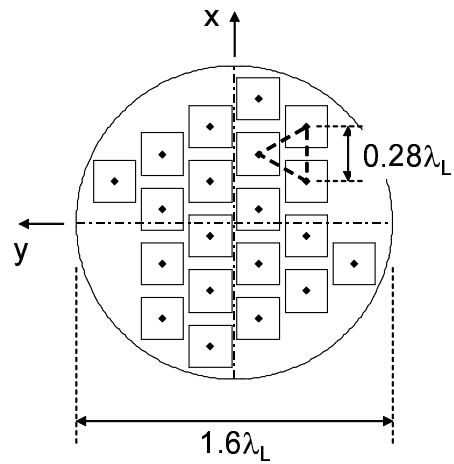


Figure 8: Layout of spiral array antenna having 20 elements

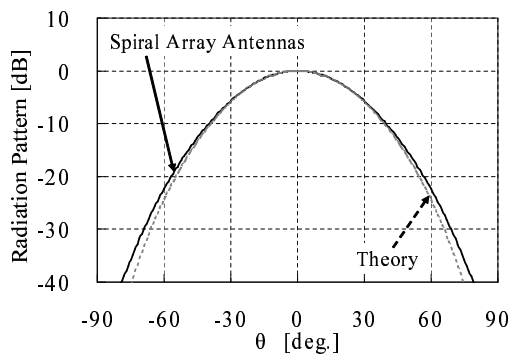


Figure 9: Array antenna pattern at f_L

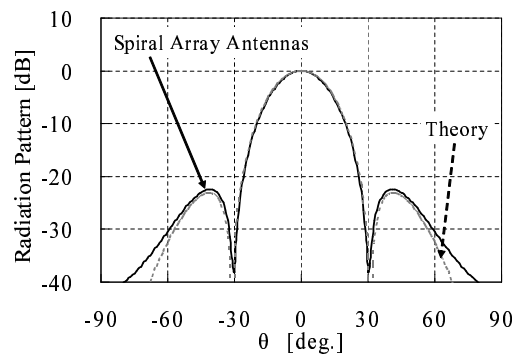


Figure 10: Array antenna pattern at $2f_L$

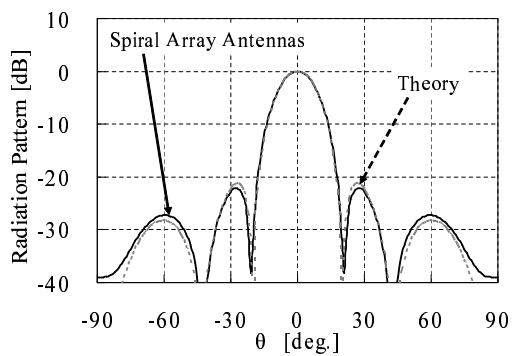


Figure 11: Array antenna pattern at $3f_L$

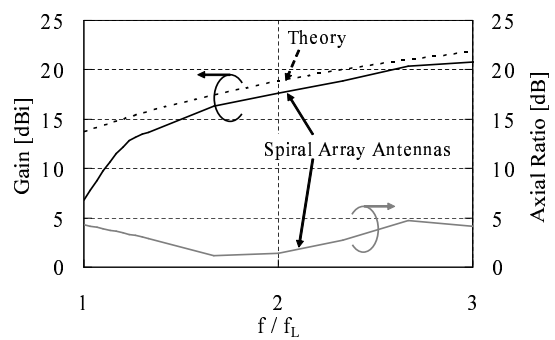


Figure 12: Antenna gain and axial ratio of array antenna